Front. Earth Sci. 2023, 17(1): 170−179
https://doi.org/10.1007/s11707-022-1042-x

RESEARCH ARTICLE

Acoustic response characteristics and sensitivity of briquette and raw coal under temperature and pressure control

Hewei ZHANG[1,2], Jian SHEN (✉)[1,2], Kexin LI[3], Xiaojie FANG[1,2], Ziwei WANG[1,2], Lei DU[4]

1 Key Laboratory of Coalbed Methane Resources and Reservoir Formation Process (Ministry of Education), China University of Mining and Technology, Xuzhou 221008, China
2 School of Resources and Geosciences, China University of Mining and Technology, Xuzhou 221116, China
3 Huabei Oilfield CBM Branch Company, Changzhi 046000, China
4 Shaanxi Coalfield Geophysical Exploration and Mapping Co., Ltd., Xi'an 710000, China

© Higher Education Press 2023

Abstract Acoustic testing is a widely used technique to measure the coal mechanical properties under high temperature and pressure *in situ* conditions. This study compared the acoustic wave characteristics of briquette and raw coal under various temperature and pressure conditions. The results show that the longitudinal wave velocity (V_p) decreases with an increasing vitrinite content. A large number of the vitrinite content enhances the process in which the temperature and pressure changed the V_p. The V_p of briquette decreases approximately linearly with the temperature compared to raw coal. The V_p of raw coal experiences initially a rapid, then gradual, and finally the moderate increasing trend with the increase in confining pressure. However, in briquette, the V_p increases approximately linearly with the confining pressure. The results indicate that the V_p is more sensitive to temperature under low confining pressure and peaks at 50°C−60°C than high confining pressure. However, the V_p is less sensitive to temperature under higher confining pressure, and the positive effect of high confining pressure is dominant. Understanding the mechanical properties of coal under high pressure and temperature develops better insight into coalbed methane (CBM) exploration from deep reservoirs.

Keywords high-rank coal, P-wave velocity, temperature, pressure, microscopic components, sensitivity

Received January 4, 2022; accepted August 31, 2022

E-mail: jianshen@cumt.edu.cn

1 Introduction

Understanding of coal reservoir parameters is necessary for the robust selection of coalbed methane (CBM) reservoir (Palmer, 2010), drilling operation (Zhu et al., 2012), reservoir reconstruction (Shi et al., 2017), and drainage mechanism (Karacan, 2009). The complex pore structure and coal cleats increase the difficulty of coalbed methane exploration and production (Şenel et al., 2001; Wei et al., 2019). In addition, the heterogeneous characteristics of coal cause difficulty in sample preparation, and it is difficult to measure the mechanical properties of coal under high temperature and pressure *in situ* conditions. Therefore, a non-destructive, fast, and representative evaluation technology is required to accelerate CBM production.

Acoustic waves are used to determine petrophysical parameters of reservoirs (Donohue et al., 2013; Cardarelli et al., 2014). However, the propagation of acoustic waves in rocks is affected by geological factors such as water, confining pressure, temperature, density (Li et al., 2021; Liu et al., 2021a), pore geometry, and mineral composition (Tandon and Gupta, 2013; Martínez-Martínez et al., 2016). The speed of acoustic waves becomes fast with the high rock density and Young's modulus (Gaviglio, 1989; Khalil and Hanafy, 2008; Antonangeli et al., 2012; Rabbel et al., 2013). Porosity and permeability are negatively correlated with the longitudinal wave velocity (V_p) (Popp and Kern, 1998; Brown et al., 2009; Wang et al., 2009; Maalej et al., 2013). Moreover, the V_p decreases with increasing temperature (Krzesińska, 2000; Punturo et al., 2005) but positively correlated with the pressure (Yang et al., 2014). In the past, acoustic waves had been used to study petrophysical

characteristics mostly of sandstone, carbonate rock, and basalt, while few studies were done on coal.

Coal is a complex organic rock with strong acoustic anisotropy (Wang et al., 2015a). The coal rank, pore distribution, carbon content, and ash yield affect the acoustic characteristics of coal. (Meng et al., 2011; Nara et al., 2011; Pan et al., 2013; Li et al., 2017; Golsanami et al., 2021). However, the physical properties of coal reservoirs under geological conditions are mainly regulated by temperature and pressure (Gao et al., 2019). Therefore, it is necessary to understand the acoustic characteristics of coal under temperature and pressure conditions. In coal, bound water, pores and cracks have a strong relationship with temperature. The bound water of coal decreases with the increase in temperature (Liu et al., 2017). The coal pores and fissures increase to varying degrees with the temperature (Yan et al., 2020; Liu et al., 2021b). Coal properties such as matrix compression and reduction of pores change under the influence of confining pressure (Yao and Han, 2008; Li et al., 2016; Shkuratnik et al., 2016; Huang et al., 2020). The influence of physical factors on the acoustic velocity of coal were discussed previously by many researchers (Meng et al., 2008). However, coal composition, temperature and pressure control effects on acoustic velocity and sensitivity were seldom analyzed.

The high-rank coals were collected from the southern Qinshui Basin and processed as raw coal and briquette. The maximum reflectance ($R_{o,max}$) of oil-immersed vitrinite and composition of these samples were measured. Moreover, the porosity and the V_p of the dried coal samples were measured under different temperature and pressure control conditions. The coal composition, temperature, and pressure effects on coal acoustic velocity were analyzed, which provides a reference for the acoustic prediction of deep coal reservoir parameters.

2 Samples and experimental methods

2.1 Sampling point and sample preparation

The raw coal samples were collected from the No. 3 coal seam of Zhulinshan Mine and Fuyanshan Mine in the southern Qinshui Basin. The coal seams are in the Shanxi Formation of the Lower Permian. The Qinshui Basin located in the central part of north China, and it is a large north-east-trending Syncline as a whole. The east wing has an inclination angle of about 10°, which is relatively gentle. The west wing is relatively steep, with an inclination angle of 10°−20°. Many secondary folds and high-angle normal faults are developed in the basin. The main coal-bearing strata in the southern Qinshui Basin are the Carboniferous-Permian Taiyuan Formation and Shanxi Formation. The thickness of the No. 3 coal seam in Shanxi Formation is in the range of 0.8−6.4 m, $R_{o,max}$ ranges from 1.3% to 4.0%, with an average of 3.2%, and the coal rank in the south is higher than in the northern region (Fig. 1).

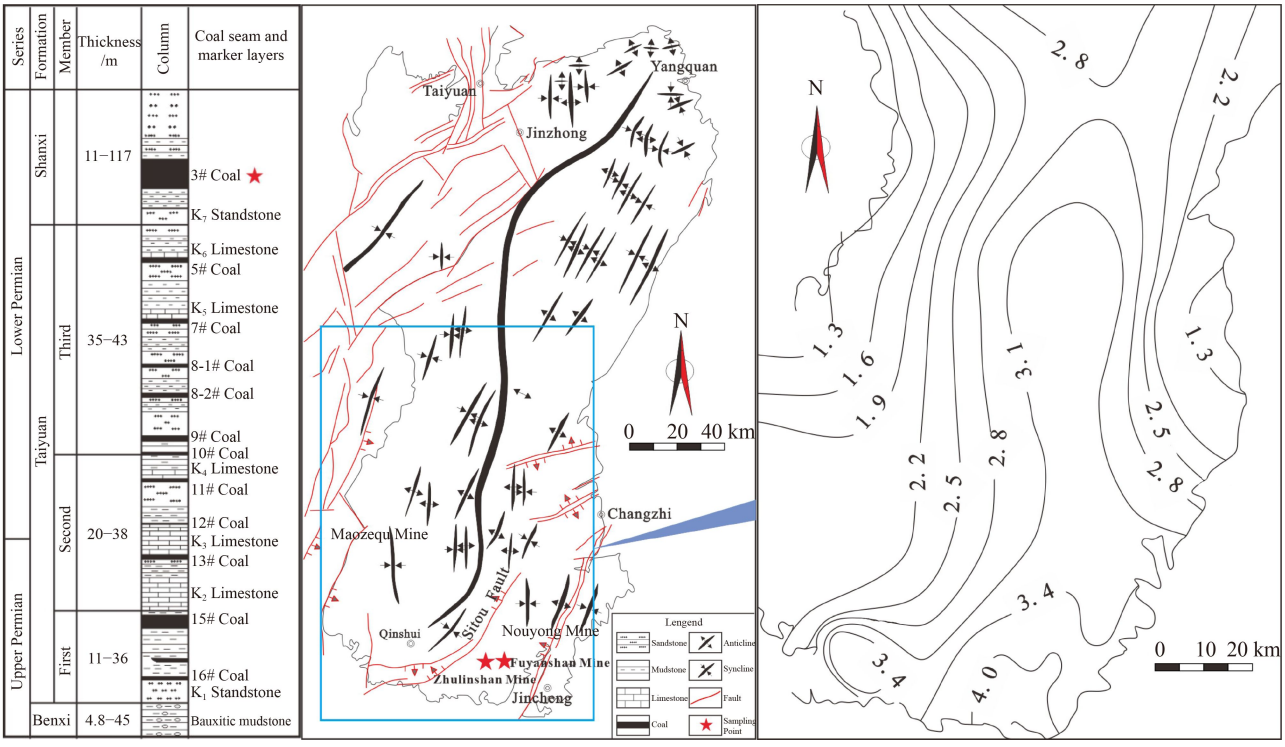

Fig. 1 Sampling location of Zhulinshan and Fuyanshan mine.

2.1.1 Briquette

The raw coal of Zhulinshan Mine was used to prepare briquette sample to study the regulating effect of maceral components on acoustic wave velocity under different temperature and pressure conditions. The process of briquette sample preparation follows specific steps.

1) The raw coal with well-developed vitrinite was preliminarily crushed to collect vitrinite strips.

2) The vitrinite strips were mechanically ground, and particles with diameters ranging from 0.12 to 0.25 mm were screened for further process.

3) The screened powdered samples were dried in the oven at a constant temperature (80°C) for more than 24 h to no longer change the quality of the samples.

4) The dried powdered sample was divided into three sub-samples named: ZJ-1, ZJ-2, and ZJ-3. These samples were individually molded into cylindrical sizes with 50 mm × 80 mm under the same experimental conditions. The remaining dried powdered samples were used for maceral component and industrial component tests at the same time.

5) The acoustic tests were performed immediately after the preparation of briquettes under different temperature and pressure conditions. Furthermore, the microscopic composition and vitrinite reflectivity of each briquette sample was also determined.

2.1.2 Raw coal

The raw coal samples from the Fuyanshan Mine were drilled along the bedding direction to get 50 mm ×100 mm sized cylinders denoted as FYS-1, FYS-2, and FYS-3. At the same time, the residual samples at the end was collected for basic experiments.

2.2 Experimental methods

Maceral analysis, $R_{o,max}$ and proximate analysis tests were performed according to corresponding standards. The maximum reflectance ($R_{o,max}$) of oil-immersed vitrinite and the maceral composition of coal were determined following ASTM standard D2798-05 and ISO7404-3 (2009). The proximate analysis of coal was done in Jiangsu Institute of Geology and Mineral Resources following the national standard (GB/T 30732-2014).

The mercury porosimeter (Poremaster 60 GT, Quantachrome Instruments, Boynton Beach, USA) was used to conduct the mercury intrusion porosimetry (MIP) test at Nanjing University of Technology. The coal samples were dried at a constant temperature of 80°C for 24 h. The maximum test pressure was about 274 MPa, and the minimum test aperture was 5.4 nm.

The acoustic wave experiment was performed at Southwest Petroleum University, using the SCMS-E high temperature and pressure core multi-parameter instrument (Fig. 2). The equipment is mainly composed of a gas pressure regulating system, a gripper, an acoustic wave instrument, a confining pressure-axial pressure system, a temperature control system and a data acquisition system. The working temperature of the equipment is between 20°C and 150°C, the accuracy is 0.5°C, the maximum confining pressure is 50 MPa, the accuracy is 0.1 MPa, and the V_p accuracy is 0.001 m/s. The average geothermal gradient in the study area is about 2.4°C/hm, and acoustic wave tests at different T-P are designed to explore the V_p response characteristics of coal seams buried at a depth of

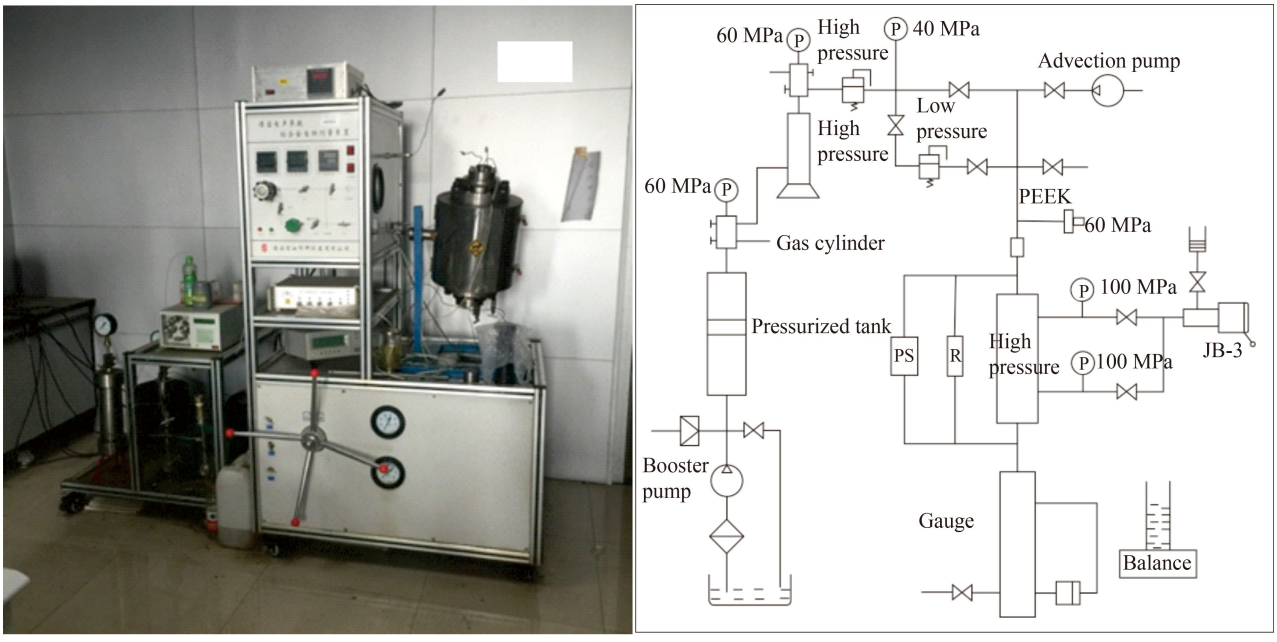

Fig. 2 SCMS-E Acoustic Measurement Equipment.

800−2000 m. The experiment was conducted at four different test temperatures (40°C, 50°C, 60°C, 70°C) and five different test pressures (7 MPa, 9 MPa, 14 MPa, 19 MPa, 24 MPa). The acoustic testing proceeds as follows.

1) Put the standard sample into the holder, load 2 MPa confining pressure, turn on the sonic pulse transmitter to measure, and record the data. Comparing the test results with the longitudinal wave properties of the standard block, the sample test can be carried out with an error of less than 1%.

2) Load the sample to be tested, turn on the heating device and raise the temperature to 40°C. After the temperature is stable, load the confining pressure to 7 MPa. After stabilization, turn on the acoustic wave transmitter to record the test data. The same temperature and pressure point were measured three times, and the average value was taken as the test result.

3) After completing one confining pressure point, slowly load the confining pressure to the next test pressure point, and repeat step 2. After all pressure points at one temperature are completed, slowly unload the confining pressure, then heat up to the next temperature point, and repeat step 2.

4) After all tests of one sample are completed, remove the pressure and temperature, and repeat steps 2 and 3.

3 Results

3.1 Basic properties

The basic properties of briquette samples (ZJ-1, ZJ-2, ZJ-3) and raw coal samples (FYS-1, FYS-2, FYS-3) are given in Table 1. The maximum reflectance of the briquette samples (2.94%−2.99%) is higher than the raw coal samples (2.29%−2.40%). The maceral composition of briquette samples is significantly different from the raw coal samples. The vitrinite content of the briquette samples (average 97.89%) is higher than the raw coal samples (average 75.09%). Both briquette and raw coal samples contain less water, low ash, and low volatile yield.

3.2 Characteristics of MIP pore structure

The mercury intrusion curve (Fig. 3(a)) shows a prominent characteristic of pores segmentation. The mercury intrusion volume increases slowly at the 50−10000 nm pore size stage, and rapidly increases at the < 50 nm pore size stage, indicating that the pores < 50 nm in all the samples are well-developed. In addition, the cumulative mercury injection curve shows that there are

Table 1 Basic properties of the samples

Sample	$R_{o,max}$	Macerals/%				Industrial components/%			
		V	I	E	M	M_{ad}	A_{ad}	V_{daf}	F_{cd}
ZJ-1	2.97	98.04	1.96	/	/	9.63	6.07	8.63	85.82
ZJ-2	2.99	97.81	2.21	/	/	4.30	5.49	12.96	82.25
ZJ-3	2.94	97.46	2.54	/	/	5.40	6.10	12.90	81.78
FYS-1	2.29	73.37	22.88	1.56	2.19	2.84	11.58	9.15	80.34
FYS-2	2.39	80.70	14.80	1.90	2.60	3.39	8.80	6.65	85.14
FYS-3	2.40	71.20	24.30	3.51	0.99	2.62	13.30	9.79	78.45

Notes: V is vitrinite content, I is inertinite content, E is exinite content, M is mineral content, M_{ad} is moisture content, A_{ad} is ash yield, V_{daf} is volatile component yield, F_{cd} is fixed carbon content.

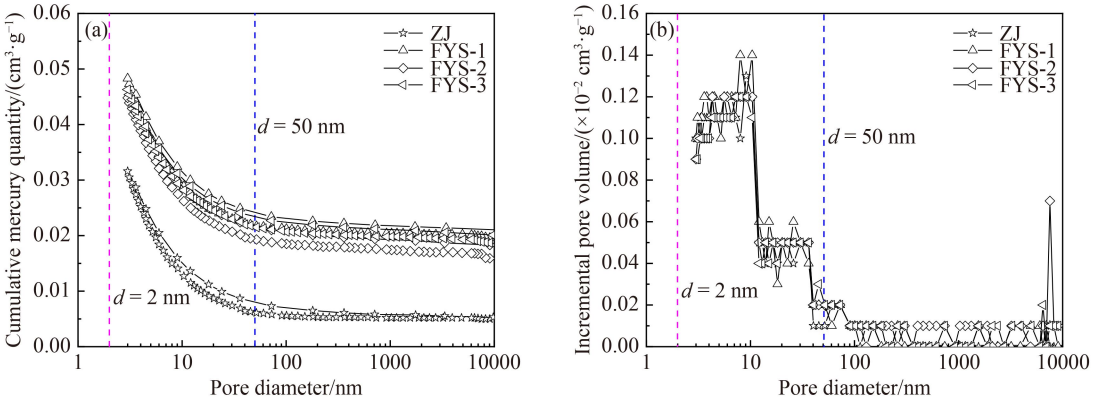

Fig. 3 MIP curves: cumulative mercury quantity (a) and incremental pore volume (b).

apparent hysteresis loops for mercury extrusion in the coal samples. The hysteresis loops overlap the mercury injection curve, indicating that most coal pores in the sample are semi-closed (Zhao et al., 2019). Figure. 3(b) shows multiple peaks of pore size distribution with the increase in pore volume. According to the IUPAC pore size classification, the coal samples have mainly mesopores (5−40 nm) and macropores (⩾ 6000 nm) (Sing and Sw, 1985).

3.3 Acoustic characteristics under temperature-pressure conditions

The porosity test results under temperature and pressure show that the measured porosity of briquette samples ranges from 42.6% to 43.2%, which is more significant than the raw coal (3.07%−6.88%). The compressional wave velocity of briquette (ZJ-1, ZJ-2, ZJ-3) under different temperature and pressure conditions are significantly lower than the raw coal (FYS-1, FYS-2, FYS-3) (Table 2).

The difference between raw coal and briquette acoustic waves under various temperature and pressure conditions shows two characteristics. 1) The range of V_p of the raw coal significantly varies than the briquette under the increase of confining pressure. However, the V_p change rate of the briquette is more significant than the raw coal (except the sample FYS-3). 2) The range and average change rate of V_p of briquette at the temperature ranging from 40°C−70°C are smaller than the raw coal.

Table 2 Experimental results of coal samples under different temperature and pressure

Sample	Porosity/%	Confining pressure/MPa	Temperature			
			40°C	50°C	60°C	70°C
			V_p/(m·s^{-1})	V_p/(m·s^{-1})	V_p/(m·s^{-1})	V_p/(m·s^{-1})
ZJ-1	43.1	7	513.32	495.87	458.02	452.26
		9	584.42	579.71	485.83	480.00
		14	761.07	740.74	715.00	697.67
		19	764.38	748.44	746.30	740.74
		24	796.46	792.17	801.48	807.21
ZJ-2	42.6	7	599.00	586.32	509.92	484.42
		9	701.07	687.02	630.47	621.58
		14	740.74	748.44	736.30	729.48
		19	835.72	825.69	815.07	811.11
		24	865.38	862.38	868.90	872.91
ZJ-3	43.2	7	584.42	495.87	489.92	485.83
		9	627.18	586.32	579.71	545.87
		14	687.02	630.47	627.18	616.58
		19	729.48	718.44	697.67	692.30
		24	814.48	807.17	800.14	805.11
FYS-1	3.07	7	1783.94	1740.81	1683.82	1629.27
		9	1829.27	1815.43	1806.23	1788.38
		14	1876.96	1857.59	1853.68	1843.32
		19	1952.37	1930.50	1927.19	1901.74
		24	2295.92	2259.89	2224.97	2095.46
FYS-2	6.88	7	1324.50	1173.40	1134.29	947.54
		9	1536.49	1444.04	1349.33	1303.60
		14	1641.00	1623.08	1604.99	1570.00
		19	1852.80	1829.27	1679.89	1665.00
		24	1953.34	1927.19	1901.74	1876.96
FYS-3	6.32	7	1093.23	1068.88	767.10	743.34
		9	1641.56	1584.36	1336.80	1312.43
		14	1720.02	1699.72	1679.89	1660.52
		19	2036.20	2007.81	1762.11	1740.81
		24	2784.22	2371.54	2095.46	2065.40

4 Discussion

4.1 Effect of maceral components on V_p

The V_p is negatively correlated with the vitrinite content (Fig. 4(a)) while positively related to the inertinite content (Fig. 4(b)) in corroboration with the findings of Liu et al. (2017) and Li et al. (2016) had discovered these same phenomena. The main reason may be the difference of pore structure and pore distribution in the raw coal.

Generally, the coal maceral composition varies with different pore and fissure types, increasing the heterogeneity of coal acoustic characteristics. The microcracks in the vitrinite are more developed than the inertinite result in the V_p decrease with the increase of vitrinite content. In addition, the V_p is also affected by factors such as coal grade, moisture content and ash yield, which greatly enhances the heterogeneity of sound wave propagation. Yao et al. (2010) also support our results by founding that the degree of micro-fracture development varies significantly with the different maceral compositions of coal.

The physical properties of briquette samples ZJ-1, ZJ-2, and ZJ-3 prepared from the same raw coal are the same. However, the V_p response characteristics of these samples vary under different temperature and pressure conditions.

Figure 5 shows that the average change rate of V_p under the confining pressure ranging from 7 MPa to 24 MPa in the briquette increases with the temperature (Fig. 5). The briquette samples with higher vitrinite content (ZJ-1, ZJ-2) have a higher change rate than the briquette sample (ZJ-3) with the lowest vitrinite content, which indicates that the briquette with higher vitrinite content is more sensitive to the temperature changes.

In Fig. 6, the average change rate of V_p under the influence of temperature ranging from 40°C to 70°C decreases with the confining pressure. The briquette samples with higher vitrinite content (ZJ-1, ZJ-2) show tremendous change and a significant average V_p change rate fluctuation curve than the ZJ-3 sample. It indicates that the briquette with higher vitrinite content is also more sensitive to changes in confining pressure than the low vitrinite briquette.

4.2 Effect of temperature on V_p

The V_p of raw coal and briquette decrease with the increase in temperature, whereas changes in V_p are more

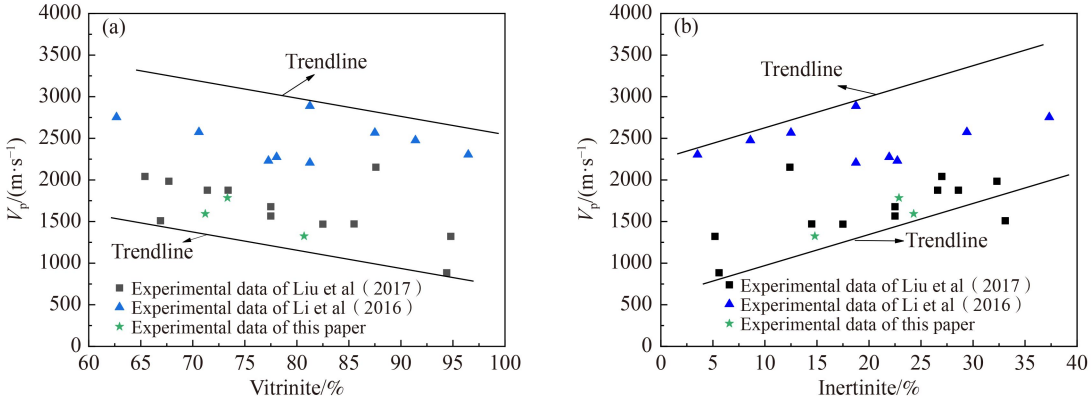

Fig. 4 Relationship between the maceral content and V_p ((a) vitrinite, (b) inertinite) in raw coal.

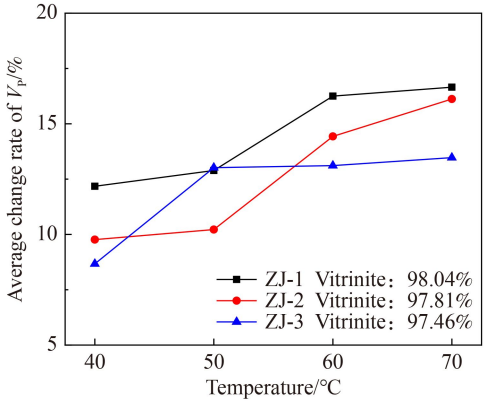

Fig. 5 The relationship between the average change rate of V_p and temperature.

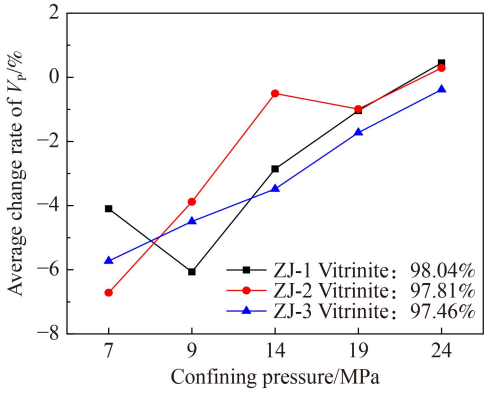

Fig. 6 The relationship between the average change rate of V_p and confining pressure.

linear in briquette (Fig. 7). Yao and Han (2008) also observed a linear trend change of V_p in coal at the temperature ranging 22°C−90°C.

The changes in the speed of sound waves with temperature depend upon the way these waves propagate in the coal sample. The coal has a complex pores and fissures, and the degree of development of pores and fissures in coal is inversely proportional to the V_p (Wang et al., 2015b). Moreover, the increase in temperature causes thermal expansion in the channels between isolated pores and other pores, increasing the total porosity of the coal. The influence of high-temperature thermal stress can also cause micro-cracks in the rock mass, which reduces the acoustic wave speed to a certain extent (Nara et al., 2011). According to Yan et al. (2020), the increase in temperature from 25°C to 65°C leads to an increase in coal porosity and a decrease in V_p, which supports our findings.

4.3 Effect of confining pressure on V_p

The confining pressure accelerates the V_p of raw coal and briquette, shown in Fig. 8, consistent with the findings of other researchers (Feng et al., 2012; Wu et al., 2015; Li et al., 2016; Liu et al., 2017). The V_p increases with the confining pressure due to the gradual closure of micro-cracks or pores (Punturo et al., 2005).

Figure 8(a) shows a rapid increase in the V_p of raw coal samples (FYS-1, FYS-2) at the confining pressure ranging from 7−9 MPa, followed by a gradual increase at the pressure ranging from 9 MPa to 19 MPa, then a moderate increase at the pressure range of 19−24 MPa. In comparison, the FYS-3 samples follow the same behavior as FYS-1 and FYS-2, except that the increase in V_p is more linear at the pressure ranging 9−14 MPa, which may be caused by differences in sample properties. Our results are in concordance with the findings of Popp and Kern (1998), which showed that the V_p increased sharply at low pressure and increased slowly under high pressure. Briquette samples (Fig. 8(b)) show comparatively the approximately linear change under the same pressure range used for raw coal.

4.4 Sensitivity of V_p to temperature and pressure

The temperature and confining pressure have opposite effects on the V_p for raw coal and briquette samples. So, which one dominates under the combined effect of the two? Therefore, the change rate of V_p is used to characterize the sensitivity of V_p to temperature and pressure.

The characteristic of the V_p change rate under the low

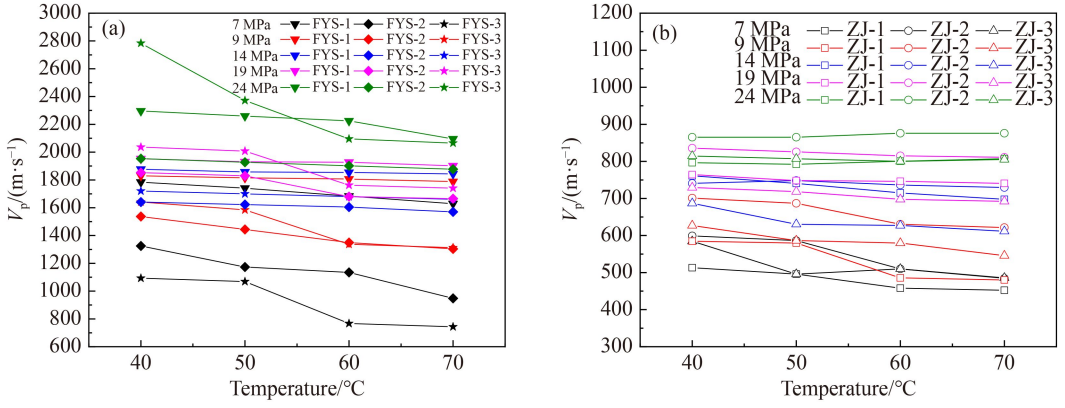

Fig. 7 Relationship between V_p and temperature of raw coal (a) and briquette (b) under different pressures.

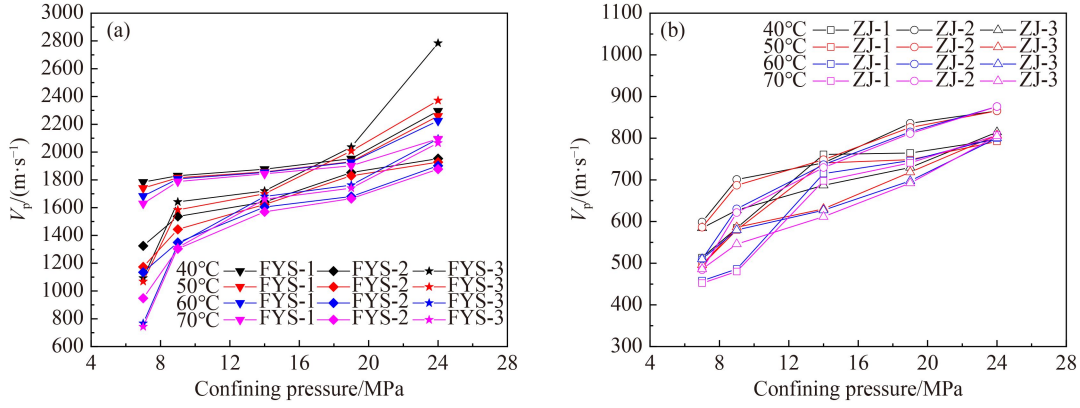

Fig. 8 Relationship between V_p and confining pressure of raw coal (a) and briquette (b) under different pressures.

confining pressure (7 MPa) shows a trend of increase followed by a decrease with the increasing temperature (Fig. 9). The rate of change of V_p varies significantly at different temperature stages and peaks at the stage of 50°C−60°C. Under high confining pressure, the change rate decreases non-significantly with the increasing temperature. The change rate of V_p of raw coal under low confining pressure (Fig. 9(a)) is significantly higher than that of briquette in general (Fig. 9(b)), and under higher confining pressure (19−24 MPa), the V_p change rate of raw coal fluctuates more than the briquette coal. The V_p increases with the temperature under the confining pressure of 24 MPa, indicating that the positive effect of the confining pressure overcomes the negative effect of temperature.

The change rate of V_p decreases with the increase in confining pressure (Fig. 10). The change rate of V_p from the raw coal decreases rapidly when the confining pressure increases from 7 MPa to 9 MPa; however, a gradual decrease is observed at other stages (Fig. 10(a)). Moreover, the difference between the rate of change of V_p at various stages of confining pressures becomes more pronounced as the temperature increases. The difference in change rate between briquette samples and the raw coal is non-significant (Fig. 10(b)).

Figure 10 indicates that the V_p is more sensitive to the changes at low temperature and confining pressure, while the positive effect of the high pressure gradually dominates when both temperature and pressure increase together. The briquette samples exhibit more stability to change in the V_p than raw coal with increased temperature and pressure.

5 Conclusions

1) The V_p is negatively correlated with the vitrinite content whereas positively correlated with the inertinite content of the coal. Under the low confining pressure, the V_p change rate of the briquette with higher vitrinite content is greater than the briquette with lower vitrinite content with the temperature increase. However, the change rate of V_p of the briquette with higher vitrinite content shows higher fluctuations than the briquette with low vitrinite content with the increasing confining pressure. Thus, it indicates that the V_p of the briquette with higher vitrinite content is more sensitive to temperature and confining pressure.

2) As the temperature increases, the coal V_p decreases. The V_p of raw coal and briquette decreases approximately

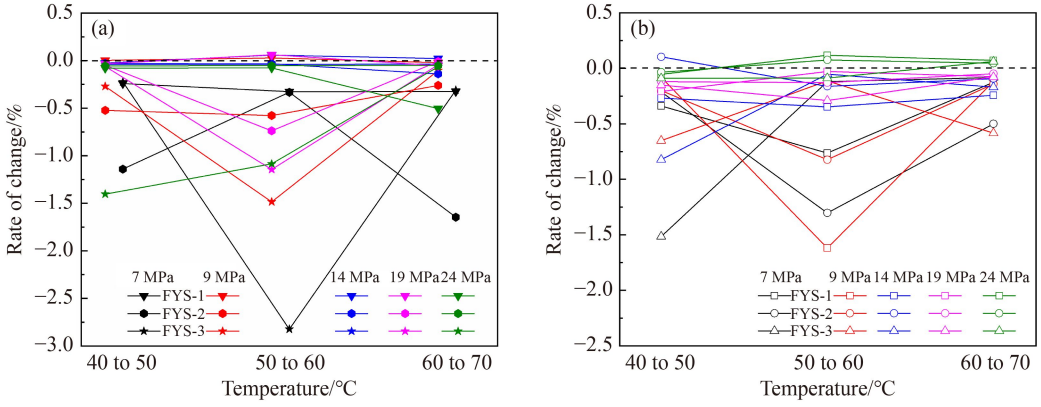

Fig. 9 Relationship between change rate of V_p of raw coal (a) and briquette (b) and temperature.

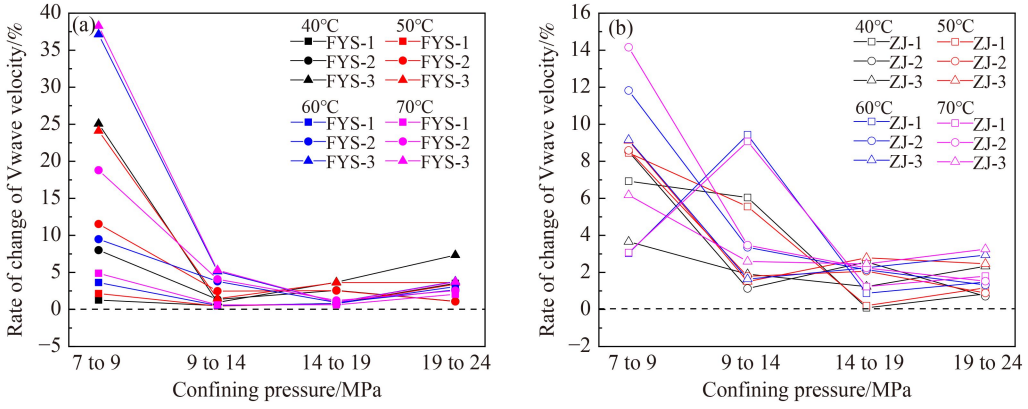

Fig. 10 Relationship between change rate of V_p of raw coal (a) and briquette (b) and confining pressure.

linearly under the pressure range of 7−24 MPa, but the change was more gradual in briquette compared to raw coal samples.

3) The V_p of raw coal experiences a rapidly increasing trend at 7−9 MPa, followed by a gradual increase at 9−19 MPa, then a moderate increase at 19−24 MPa, whereas the V_p of briquette increases approximately linearly with the confining pressure.

4) The V_p is more sensitive to temperature under low confining pressure and peaks at 50°C−60°C. The V_p is less sensitive to temperature under high confining pressure, while the positive effect of high confining pressure is dominant. At a specific temperature, the sensitivity of V_p to low confining pressure is more significant than at high confining pressure. In addition, the sensitivity of V_p to the confining pressure increases with the temperature.

Acknowledgment This research was financially supported by the National Natural Science Foundation of China (Grant Nos. 42072191 and 42130802), the Shanxi Science and Technology Plan Announced Bidding Project (No. 20201101003), the China Huaneng Group Scicence and Technology Project (No. HNKJ20-H87), the Qing Lan Project of Jiangsu Province, and Priority Academic Program Development of Jiangsu Higher Education Institutions (PPAD). Finally, we are very grateful to Khadija for her help on the language of the paper.

References

Antonangeli D, Komabayashi T, Occelli F, Borissenko E, Walters A C, Fiquet G, Fei Y (2012). Simultaneous sound velocity and density measurements of hcp iron up to 93 GPa and 1100 K: an experimental test of the Birch's law at high temperature. Earth Planet Sci Lett, 331: 210–214

Brown D, Llana-Funez S, Carbonell R, Alvarez-Marron J, Marti D, Salisbury M (2009). Laboratory measurements of P-wave and S-wave velocities across a surface analog of the continental crust–mantle boundary: Cabo Ortegal, Spain. Earth Planet Sci Lett, 285(1–2): 27–38

Cardarelli E, Cercato M, De Donno G (2014). Characterization of an earth-filled dam through the combined use of electrical resistivity tomography, P-and SH-wave seismic tomography and surface wave data. J Appl Geophys, 106: 87–95

Donohue S, Forristal D, Donohue L A (2013). Detection of soil compaction using seismic surface waves. Soil Tillage Res, 128: 54–60

Feng Z, Mingjie X, Zhonggao M, Liang C, Zhu Z, Juan L (2012). An experimental study on the correlation between the elastic wave velocity and microfractures in coal rock from the Qingshui Basin. J Geophys Eng, 9(6): 691–696

Gao Y, Gao F, Dong G, Yan W, Yang X (2019). The mechanical properties and fractal characteristics of the coal under temperature-gas-confining pressure. Therm Sci, 23(Suppl 3): 789–798

Gaviglio P (1989). Longitudinal waves propagation in a limestone: the relationship between velocity and density. Rock Mech Rock Eng, 22(4): 299–306

Golsanami N, Zhang X, Yan W, Yu L, Dong H, Dong X, Cui L, Jayasuriya M N, Fernando S G, Barzgar E (2021). NMR-based study of the pore types' contribution to the elastic response of the reservoir rock. Energies, 14(5): 1513–1538

Huang L, Liu X, Yan S, Xiong J, He H, Xiao P (2020). Experimental study on the acoustic propagation and anisotropy of coal rocks. Petroleum, 8(1): 31–38

Karacan C Ö (2009). Reservoir rock properties of coal measure strata of the Lower Monongahela Group, Greene County (Southwestern Pennsylvania), from methane control and production perspectives. International Journal of Coal Geology, 78(1): 47–64

Khalil M H, Hanafy S M (2008). Engineering applications of seismic refraction method: a field example at Wadi Wardan, Northeast Gulf of Suez, Sinai, Egypt. J Appl Geophys, 65(3–4): 132–141

Krzesińska M (2000). Correlation of absolute temperature coefficients of ultrasonic velocity in solutions of dilute coal and lignite extracts with molecular masses. Fuel, 79(15): 1907–1912

Li N, Fu L Y, Yang J, Han T (2021). On three-stage temperature dependence of elastic wave velocities for rocks. J Geophys Eng, 18(3): 328–338

Li Q, Chen J, He J (2016). Laboratory measurements of the acoustic velocities and elastic property of coal rocks and their link with microfeatures. SEG Technical Program Expanded Abstracts 2016. Society of Exploration Geophysicists, 3359–3363

Li X, Meng Y, Yang C, Nie B, Chen X (2017). Effects of pore structure on acoustic wave velocity of coal samples. J Nanosci Nanotechnol, 17(9): 6532–6538

Liu J, Kang Y, Chen M, You L, Zhang T, Gao X, Chen Z (2021a). Investigation of enhancing coal permeability with high-temperature treatment. Fuel, 290(6): 120082

Liu J, Liu D, Cai Y, Gan Q, Yao Y (2017). Effects of water saturation on P-wave propagation in fractured coals: an experimental perspective. J Appl Geophys, 144: 94–103

Liu P, Fan L, Fan J, Zhong F (2021b). Effect of water content on the induced alteration of pore morphology and gas sorption/diffusion kinetics in coal with ultrasound treatment. Fuel, 306: 121752

Maalej S, Lafhaj Z, Bouassida M (2013). Micromechanical modelling of dry and saturated cement paste: porosity assessment using ultrasonic waves. Mech Res Commun, 51: 8–14

Martínez-Martínez J, Fusi N, Galiana-Merino J J, Benavente D, Crosta G B (2016). Ultrasonic and X-ray computed tomography characterization of progressive fracture damage in low-porous carbonate rocks. Eng Geol, 200: 47–57

Meng Z P, Liu C Q, He X h, Zhang N (2008). Experimental research on acoustic wave velocity of coal measures rocks and its influencing factors. J Mining Safety Eng. 25(4): 389–393 (in Chinese)

Meng Z, Zhang J, Wang R (2011). *In-situ* stress, pore pressure and stress-dependent permeability in the southern Qinshui Basin. Int J Rock Mech Min Sci, 48(1): 122–131

Nara Y, Meredith P G, Yoneda T, Kaneko K (2011). Influence of macro-fractures and micro-fractures on permeability and elastic wave velocities in basalt at elevated pressure. Tectonophysics, 503(1–2): 52–59

Palmer I (2010). Coalbed methane completions: a world view. Int J

Coal Geol, 82(3–4): 184–195

Pan J, Meng Z, Hou Q, Ju Y, Cao Y (2013). Coal strength and Young's modulus related to coal rank, compressional velocity and maceral composition. J Struct Geol, 54: 129–135

Popp T, Kern H (1998). Ultrasonic wave velocities, gas permeability and porosity in natural and granular rock salt. Phys Chem Earth, 23(3): 373–378

Punturo R, Kern H, Cirrincione R, Mazzoleni P, Pezzino A (2005). P- and S-wave velocities and densities in silicate and calcite rocks from the Peloritani Mountains, Sicily (Italy): the effect of pressure, temperature and the direction of wave propagation. Tectonophysics, 409(1–4): 55–72

Rabbel W, Kaban M, Tesauro M (2013). Contrasts of seismic velocity, density and strength across the Moho. Tectonophysics, 609: 437–455

Şenel I G, Guruz A G, Yucel H, Kandas A W, Sarofim A F (2001). Characterization of pore structure of Turkish coals. Energy Fuels, 15(2): 331–338

Shi Q, Qin Y, Li J, Wang Z, Zhang M, Song X (2017). Simulation of the crack development in coal without confining stress under ultrasonic wave treatment. Fuel, 205: 222–231

Shkuratnik V, Nikolenko P V, Koshelev A (2016). Stress dependence of elastic P-wave velocity and amplitude in coal specimens under varied loading conditions. J Min Sci, 52(5): 873–877

Sing K S W, Everett D H, Haul R A W, Moscou L, Pierotti R A, Rouquédrol J, Siemieniewska T (1985). Reporting physisorption data for gas/solid systems with special reference to the determination of surface area and porosity (Recommendations 1984). Pure Appl Chem, 57(4): 603–619

Tandon R S, Gupta V (2013). The control of mineral constituents and textural characteristics on the petrophysical & mechanical (PM) properties of different rocks of the Himalaya. Eng Geol, 153: 125–143

Wang H, Pan J, Wang S, Zhu H (2015a). Relationship between macro-fracture density, P-wave velocity, and permeability of coal. J Appl Geophys, 117: 111–117

Wang J H, Hung J H, Dong J J (2009). Seismic velocities, density, porosity, and permeability measured at a deep hole penetrating the Chelungpu fault in central Taiwan. J Asian Earth Sci, 36(2–3): 135–145

Wang Y G, Li M G, Chen B B, Dai S (2015b). Experimental study on ultrasonic wave characteristics of coal samples under dry and water saturated conditions. J China Coal Soc, 40(10): 2445–2450

Wei Q, Li X, Zhang J, Hu B, Zhu W, Liang W, Sun K (2019). Full-size pore structure characterization of deep-buried coals and its impact on methane adsorption capacity: a case study of the Shihezi Formation coals from the Panji deep area in Huainan Coalfield, southern north China. J Petrol Sci Eng, 173: 975–989

Wu H, Dong S, Li D, Huang Y, Qi X (2015). Experimental study on dynamic elastic parameters of coal samples. Int J Min Sci Technol, 25(3): 447–452

Yan M, Zhang Y, Lin H, Li J, Qin L (2020). Effect on liquid nitrogen impregnation of pore damage characteristics of coal at different temperatures. J China Coal Soc, 45(08): 2819–2823

Yang X, Yang Y, Chen J (2014). Pressure dependence of density, porosity, compressional wave velocity of fault rocks from the ruptures of the 2008 Wenchuan earthquake, China. Tectonophysics, 619: 133–142

Yao Q, Han D H (2008). Acoustic properties of coal from lab measurement. SEG Tech Prog Exp Abstr, 27(1): 1815–1819

Yao Y, Liu D, Tang D, Tang S, Huang W (2010). Influence and control of coal petrological composition on the development of microfracture of coal reservoir in the Qinshui Basin. J China U Min Tech, 39(1): 6–13 (in Chinese)

Zhao J, Qin Y, Shen J, Zhou B, Li G, Li G (2019). Effects of pore structures of different maceral compositions on methane adsorption and diffusion in anthracite. Appl Sci (Basel), 9(23): 5130

Zhu R X, Yang J H, Wu F Y (2012). Timing of destruction of the North China Craton. Lithos, 149: 51–60